Contribution from the Departments of Chemistry, Faculty of Science, Hokkaido University, Sapporo 060, Japan, and College of Humanities and Sciences, Nihon University, Sakurajosui, Setagaya-ku, Tokyo 156, Japan

Mesomorphic Property and Orientational Order in the Nematic Phases of Nickel(II) and Oxovanadium(IV) Complexes of *N*-Salicylidene-*n*-propylamine Derivatives[1]

Naomi Hoshino,*[2a] Akira Kodama,[2a] Tomoko Shibuya,[2a] Yoshio Matsunaga,[2a] and Seiichi Miyajima[2b]

Received December 26, 1990

Homologous series of new metallonematogens, bis[4-((4-alkoxybenzoyl)oxy)-*N*-*n*-propylsalicylaldiminato]nickel(II) and -oxovanadium(IV), have been synthesized and their thermotropic mesomorphism has been characterized by thermal analysis. All of the nickel(II) complexes prepared exhibit enantiotropic nematic phases over temperature ranges between 158–230 °C (melting points) and 160–253 °C (clearing points). Corresponding oxovanadium(IV) complexes are also nematogenic, but the thermal stability of the nematic phases is much lower as indicated by their clearing temperatures being depressed by 51 °C on the average. Orientational order of a nickel(II) complex in its nematic phase was investigated by means of ^{1}H NMR spectroscopy, and the results showed that the species has a more or less normal nematic order. The oxovanadium(IV) congener was dissolved in the nickel(II) nematic host and studied by ESR spectral analysis. The results for this and related oxovanadium(IV) probes have shown that the central chelate cores of these molecules are highly oriented. It has also been revealed by ^{1}H NMR measurements that the nematogenic nickel(II) complex used in these experiments shows some association phenomenon in solution.

Introduction

Thermotropic liquid crystals containing transition-metal elements (metallomesogens) have recently attracted much attention.[3-10] Our interest in metallomesogens lies in the possibilities of controlling alignment and orientation of metal complexes in their mesophases and of generating liquid crystalline materials of unconventional structures and properties. Both of these aspects would owe much to the kind of metal atoms incorporated. Transition-metal bischelates of Schiff bases are suited to the purpose of testing these possibilities due to their synthetic ease in substitution of the central metal atom as well as of peripheral groups.

Examples reported in the last couple of years favorably employ (*p*-alkoxybenzoyl)oxy substituents as terminal groups attached to either a (1) bis[*N*-arylsalicylaldiminato]copper(II)[4-6] and -oxovanadium(IV)[7] or a (2) bis[*N*-alkylsalicylaldiminato]nickel(II),[8] -copper(II),[8-10] and -oxovanadium(IV)[7] framework. The mesophases identified so far are nematic and/or smectic C, and the latter phase tends to emerge as the terminal alkoxy chains in type 1 species or *N*-alkyl chains in type 2 species are elongated. The role of the metal atoms has not been studied in a systematic fashion. Meanwhile, our previous work on a series of bis[4-((4-alkoxybenzoyl)oxy)-N-*n*-propylsalicylaldiminato]copper(II) complexes[10] has shown that, with this relatively small *N*-alkyl group, the phase behavior is quite straightforward and the entire series (from butoxy to octadecyloxy homologues) is purely nematogenic while bringing melting temperatures down to about 140 °C. This has prompted us to prepare a new series of nickel(II) and oxovanadium(IV) analogues, NiL_2 and VOL_2. They also proved to show only nematic phases; their thermal stabilities and degrees of order are compared in this paper. We also wish to report on investigations into the orientational order in the nematic phases of these complexes by means of magnetic resonance spectroscopies.

Table I. Mesomorphic Transition Temperatures (°C) and Enthalpies (ΔH/kJ mol^{-1})[a] for NiL_2 and VOL_2

	NiL_2					VOL_2		
n	K_2	K_1[b]	N	I	K_1[b]	N		I
4		· 230 (69)	· 253 (5.0)	·				
5		· 217 (62)	· 241 (4.1)	·	·	203 (50)		·
6		· 202 (60)	· 231 (4.1)	·	· 163 (53)	·	173 (1.9)	·
7		· 190 (62)	· 221 (2.9)	·	· 153 (46)	·	161 (1.5)	·
8		· 183 (66)	· 212 (2.7)	·	· 151 (56)	·	156 (1.5)	·
9		· 164 (66)	· 205 (2.4)	·	· 131 (46)	·	149 (1.4)	·
10		· 163 (69)	· 200 (2.2)	·	· 128 (53)	·	145 (1.3)	·
11		· 160 (68)	· 192 (1.9)	·	· 125 (52)	·	141 (1.2)	·
12		· 164 (78)	· 186 (1.9)	·	· 134 (68)	·	136 (1.2)	·
14	· 83 (17)	· 164 (61)	· 176 (1.8)	·	· 132 (73)	(·	129) (1.1)	·
16	· 113 (23)	· 161 (55)	· 167 (1.7)	·	· 127 (71)	(·	125) (1.2)	·
18	· 149 (29)	· 158 (59)	· 160 (1.8)	·	· 124 (78)	(·	121) (1.5)	·

[a] Listed below each transition temperature. Parenthesized temperatures indicate monotropic transitions. [b] Most stable crystalline form. Solid–solid transition and melting enthalpies were determined with annealed specimens for n = 14, 16, and 18 homologues of NiL_2 and n = 7, 9, 10, and 18 homologues of VOL_2.

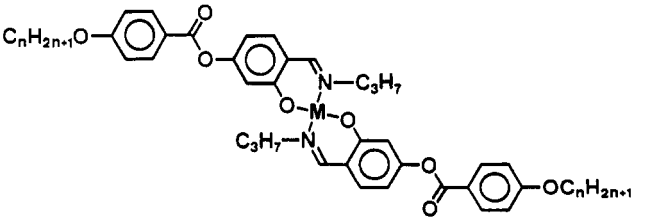

NiL_2: M = Ni, n = 4 - 12,14,16,18

VOL_2: M = VO, n = 5 - 12,14,16,18

Results and Discussion

Mesomorphic Properties. Mesomorphic phase-transition behaviors of the homologous series of NiL_2 and VOL_2 complexes

(1) A part of this work was presented at the 13th International Liquid Crystals Conference, Vancouver, Canada, July 1990.

(2) (a) Hokkaido University. (b) Nihon University.

(3) Maitlis, P. M.; Bruce, D. W.; Dhillon, R.; Dunmur, D. A.; Fanizzi, F. P.; Hunt, S. E.; Le Lagadec, R.; Lalinde, E.; Orr, R.; Rourke, J. P.; Salt, N. J. S.; Stacey, J. P.; Styring, P. *New J. Chem.* **1990**, *14*, 549–551.

(4) Bayle, J.-P., Bui, E.; Perez, F.; Courtieu, J. *Bull. Soc. Chim. Fr.* **1989**, 532–536.

(5) Hoshino, N.; Murakami, H.; Matsunaga, Y.; Inabe, T.; Maruyama, Y. *Inorg. Chem.* **1990**, *29*, 1177–1181.

(6) Marcos, M.; Romero, P.; Serrano, J. L.; Barberá, J.; Levelut, A. M. *Liq. Cryst.* **1990**, *7*, 251–259.

(7) Serrano, J. L.; Romero, P.; Marcos, M.; Alonso, P. J. *J. Chem. Soc., Chem. Commun.* **1990**, 859–861.

(8) Marcos, M.; Romero, P.; Serrano, J. L. *J. Chem. Soc., Chem. Commun.* **1989**, 1641–1643.

(9) Caruso, U.; Roviello, A.; Sirigu, A. *Liq. Cryst.* **1990**, *7*, 431–438.

(10) Hoshino, N.; Hayakawa, R.; Shibuya, T.; Matsunaga, Y. *Inorg. Chem.* **1990**, *29*, 5129–5131.

0020-1669/91/1330-3091$02.50/0

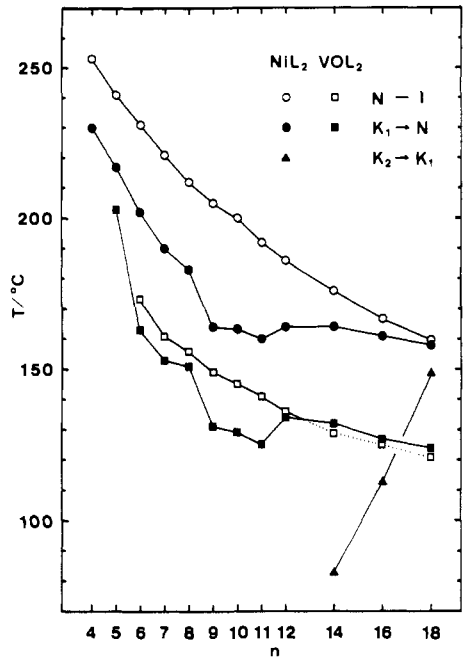

Figure 1. Plots of phase transition temperatures versus terminal alkyl chain length (n) for NiL_2 and VOL_2.

were examined by polarizing microscopic observation, and the thermodynamic parameters were determined by differential scanning calorimetry. Table I summarizes the mesomorphic transition temperatures and enthalpy changes. Here K,[11] N, and I denote crystalline, nematic, and isotropic phases, respectively, and each homologue is designated by the number of carbon atoms in the terminal alkyl chains, n. It should be noted that all of the complexes newly prepared except for VOL_2 (n = 5) exhibit nematic phases just as their copper(II) congeners do.[10] The phases of n = 14, 16, and 18 homologues of VOL_2 can be observed by supercooling the isotropic melts (monotropic transition), but VOL_2 (n = 5) seems to decompose somewhat upon melting. The observed phases displayed marble textures characteristic of nematic phases under a crossed polarizing microscope. The magnitude of isotropization enthalpies is also in the known range for other nematic materials.[12]

Figure 1 gives a graphic comparison of the phase behaviors for NiL_2 and VOL_2. It is seen that both melting ($K_1 \rightarrow N$) and clearing (N–I) temperatures as a function of n look very much alike between these series. In fact, taking into account also the case of CuL_2 reported in ref 10, the chain length dependence of the phase-transition temperatures of all three series assume similar functional forms; the melting point falls at the beginning and then tends to level off at $n \geq 9$ as the series is ascended and the clearing point simply decreases gradually all the way. If the same homologous members of NiL_2, CuL_2, and VOL_2 are compared with one another, the clearing point decreases upon substitution of Ni → Cu → VO by 27 and 25 °C and the melting point by 29 and 5 °C, on the average of 10 homologues of $n \geq 6$. The sequence of nematic thermal stability, $NiL_2 > CuL_2 > VOL_2$, seems to correspond to that of the planarity of chelate structure. Copper(II) complexes have a less anisotropic electronic configuration and are presumably more susceptible to static tetrahedral distortion than nickel(II) complexes.[13] The VOL_2 complex is most likely to have square-pyramidal geometry at the center,[14] and extrusion of the oxo bond would increase intermolecular separation in its nematic phase. Axial coordinative interaction (V–O···V–O···) may, however, become operative when molecular rotation ceases upon crystallization so that the melting temperature is maintained not far below that of CuL_2.

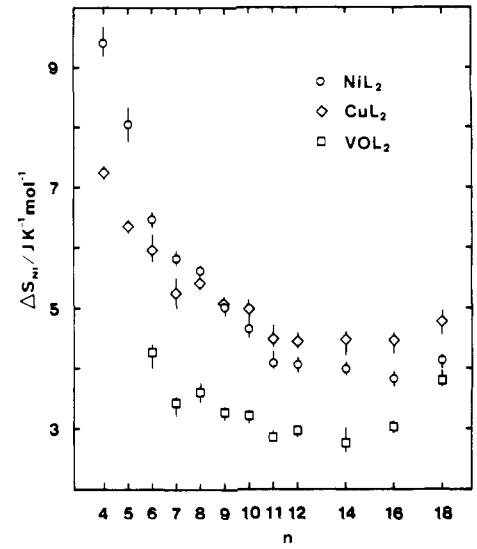

Figure 2. Plots of N–I transition entropies versus terminal alkyl chain length (n) for NiL_2, CuL_2,[10] and VOL_2.

The choice of metal atoms is thus important for the thermal stability of mesophases in the metallonematogens under discussion. They can be regarded as a molecular entity comprising a rigid chelate core, which tends to align, and flexible alkyl tails, which are more or less fluid. The degree of order in the mesophase as the outcome of this balance should be reflected in N–I transition entropy, ΔS_{NI}. In Figure 2 are plotted values of ΔS_{NI} for the series NiL_2, CuL_2,[10] and VOL_2. Variation among the three series in their ΔS_{NI} versus n relationships is clearly visible, although we cannot rely heavily on the absolute values of ΔS_{NI} due to the difficulty in accurate heat measurement.[15] Assuming that the entropies in isotropic liquid state are equal for all of the species, the degrees of order are similar in the nematic phases of NiL_2 and CuL_2; lower homologues of the former appear to be of higher order but the situation seems to reverse as the series are ascended. All of the homologues of VOL_2 are less ordered in comparison, but here again the complexes with long alkyl chains seem to start aligning better.

Microscopic Orientational Order in the Nematic Phase. The above thermodynamic parameters suggest that the metal chelate moieties of the present mesogens play a predominant role in forming the nematic phases, but their degrees of order depend on the details of molecular constitution. It is interesting, therefore, to look further into the microscopic order on the molecular level.

The liquid crystalline state is characterized by long-range orientational order, and the molecules tend to align with their long axes parallel to a given direction, which is called the director. A magnetic field can be used to align the director parallel to the field direction, yielding a macroscopically oriented sample. Nickel(II) and oxovanadium(IV) complexes similar to our NiL_2 and VOL_2 have been reported to have positive anisotropies in magnetic susceptibility,[7,8] conforming to the above orientation condition, while copper(II) analogues[6,8] tend to align with their short molecular axes parallel to the magnetic field. Therefore, a diamagnetic NiL_2 complex was subjected to ^1H NMR spectral analysis of dipolar splitting of its phenyl protons, while ESR vanadium hyperfine interaction was analyzed for its VOL_2 congener and analogues dissolved in the NiL_2 host. The aim was to determine the orientational order parameter, which describes the

(11) Most of the solids, as isolated from solution, were more or less polymorphous. Solid–solid transition and melting enthalpies for stable crystalline forms were confirmed or determined with annealed specimens whenever anomaly is detected on DSC thermograms.

(12) Demus, D.; Diele, S.; Grande, S.; Sackmann, H. In *Advances in Liquid Crystals*; Brown, G. H., Ed.; Academic Press: New York, 1983, Vol. 6, pp 1–107.

(13) Knoch, R.; Wilk, A.; Wannowius, K. J.; Reinen, D.; Elias, H. *Inorg. Chem.* **1990**, *29*, 3799–3805.

(14) Bruins, D.; Weaver, D. L. *Inorg. Chem.* **1970**, *9*, 130–135.

(15) Ranges of values calculated from several determinations of ΔH_{NI} are given in Figure 2, whereas the numbers of ΔH_{NI} in Table I are rounded averages.

degree of alignment of the long molecular axes relative to the director. It was anticipated that, when the VOL_2 congener is used as a paramagnetic probe, measured order would reflect precisely that of the NiL_2 host, owing to the close similarity in their molecular structures.

A theoretical framework is given first for local magnetic interactions observed by the NMR and ESR spectroscopies in the liquid crystalline state.[16] The magnetic interaction tensor **M** (the nuclear dipole–dipole coupling tensor **D** for NMR and the hyperfine coupling tensor **A** for ESR) is defined with respect to the principal axes fixed on a molecule. Namely, when the external magnetic field is applied parallel to these principal axes, observed spectral splittings are simply the diagonal elements of **M** along these axes. When the applied field makes a certain angle to these axes, the splitting can be calculated by means of transformation of coordinate systems

$$\Delta\nu = \sum_{\alpha}\sum_{\beta} l_{Z\alpha} l_{Z\beta} M_{\alpha\beta} \quad (1)$$

where α and β designate the molecule-fixed principal axes, and $l_{Z\alpha}$ and $l_{Z\beta}$ are the elements of the transformation matrix changing the molecular frame to the laboratory frame. The Z axis in the latter is taken parallel to the external magnetic field. The present methods utilize the fact that fast molecular motion in a mesophase averages out the matrix elements leading to a reduced splitting. A general description of this situation given by Saupe[17] employs a 3 × 3 traceless ordering matrix **S**, the elements of which are defined as

$$S_{\alpha\beta} = \langle 3 \cos\theta_\alpha \cos\theta_\beta - \delta_{\alpha\beta}\rangle/2 \quad (2)$$

where θ_α and θ_β are the angles between the principal axes and the director, and $\delta_{\alpha\beta}$ is Kronecker's δ. The director is forced to align parallel to the Z axis for mesogens having positive magnetic anisotropy, and then the matrix elements in eq 1 are simply the direction cosines of θ_α and θ_β. The partially averaged splitting is therefore given by eq 3 using the expression in eq 2. Here the

$$\langle\Delta\nu\rangle = (1/3)\,\mathrm{Tr}\,\mathbf{M} + (2/3)\sum_{\alpha} S_{\alpha\alpha} M_{\alpha\alpha} \quad (3)$$

angle brackets denote time and ensemble averages. In order to determine the scalar order parameter S in the nematic phase, one needs to perform another transformation from the symmetry axes of the molecule (principal axes of inertia, designated by j and k) to the principal axes of the local magnetic interaction

$$S_{\alpha\alpha} = \sum_{j}\sum_{k} l_{\alpha j} l_{\alpha k} S_{jk} \quad (4)$$

Substituting into eq 3

$$\langle\Delta\nu\rangle = (1/3)\,\mathrm{Tr}\,\mathbf{M} + (2/3)\sum_{\alpha}\sum_{j}\sum_{k} l_{\alpha j} l_{\alpha k} S_{jk} M_{\alpha\alpha} \quad (5)$$

Molecules in the usual nematic liquid crystals execute fast rotational diffusion around their long molecular axes (1 axis), and this makes S_{jk} axially symmetric. Then the transformation is simplified to $S_{\alpha\alpha} = P_2(l_{\alpha 1})S_{11}$, where P_2 denotes the second Legendre polynomial. The single scalar order parameter S is defined as $S = S_{11} = \langle P_2(\cos\theta_1)\rangle$ and eq 5 now becomes

$$\langle\Delta\nu\rangle = (1/3)\,\mathrm{Tr}\,\mathbf{M} + (2/3)S\sum_{\alpha} P_2(l_{\alpha 1}) M_{\alpha\alpha} \quad (6)$$

In the case of NMR of two-spin systems, the dipolar coupling tensor **D** is always traceless and has uniaxial symmetry around the interproton vector, p. Hence the three principal components are $-(1/2)D_{pp}$, $-(1/2)D_{pp}$, and D_{pp}, and they can be calculated by the definition $D_{pp} = (3/2\pi)\gamma^2\hbar r^{-3}$, where γ is the magnetogyric ratio for the proton and r is the distance between the interacting protons. Using this symmetry property, eq 6 for the NMR analysis may be given in the form

$$\langle\Delta\nu\rangle_N = P_2(l_{p1})SD_{pp} = (3/2\pi)\gamma^2\hbar r^{-3} P_2(l_{p1})S \quad (7)$$

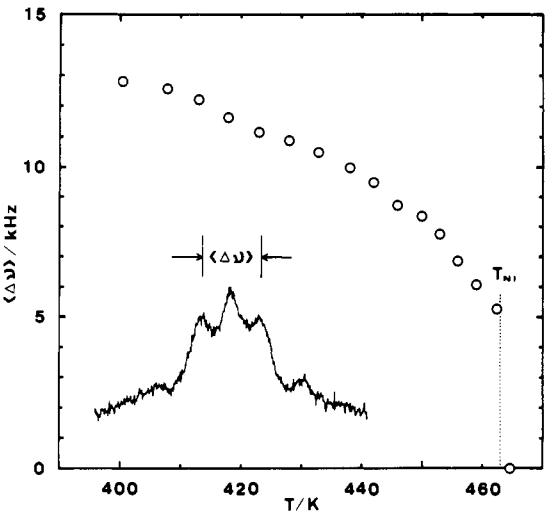

Figure 3. ^{1}H NMR dipolar splitting for NiL_2 (n = 11) as a function of temperature.

where $l_{p1} = \cos\phi$, and ϕ is the angle between the p vector and the 1 axis.

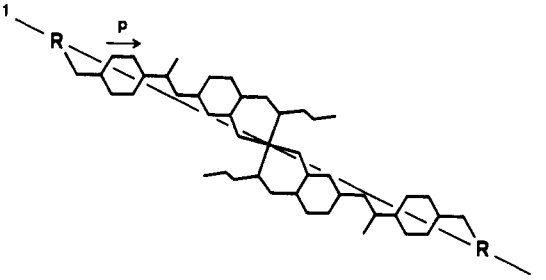

We now proceed to analyze the results of the NMR experiment with NiL_2 (n = 11) as an example. The observed spectra are exemplified by one shown in the inset of Figure 3, which was recorded at 173 °C. It consists of five peaks, the central one of which is thought to come from protons in the alkyl chains. The other four or two doublets indicate that some of the p vectors are distributed in nonspherical fashions; the inner major doublet can be ascribed to the ortho protons of the benzene rings.[18] The spacings of these peaks are plotted in Figure 3 as a function of temperature. Since $\langle\Delta\nu\rangle_N$ is directly proportional to S, the plot below T_{NI} represents the temperature dependence of the order parameter as well. The geometrical factors are estimated to be r = 0.245 nm and $\phi = 25 \pm 5°$ for NiL_2 (n = 11) from its molecular model. Values of S calculated for $\phi = 25°$ are plotted against reduced temperature, T/T_{NI}, in Figure 4.

Figure 4 also compiles data for the orientational order parameters of oxovanadium(IV) probes in NiL_2 (n = 11). In the case of ESR hyperfine interactions, the tensor **A** includes both isotropic (a**E**) and anisotropic (**A**′ = **A** − a**E**) parts, where $a = (1/3)\,\mathrm{Tr}\,\mathbf{A}$, and **E** is the identity matrix. Hyperfine spacing observed in a mesophase, $\langle\Delta\nu\rangle_E$, for a probe dissolved in a uniaxial nematic liquid crystal is derived from eq 6 by choosing appropriate principal axes, x, y, and z

$$\langle\Delta\nu\rangle_E = a + P_2(l_{z1})SA'_{zz} + (1/3)[P_2(l_{x1}) - P_2(l_{y1})]S(A'_{xx} - A'_{yy}) \quad (8)$$

Although the location of the xyz coordinate is not known for our complexes, it seems natural to assume that the z axis lies along the V=O bond direction,[19] and therefore $P_2(l_{z1})$ is set equal to $-1/2$. Unlike the pairwise dipolar interaction in NMR, the tensor **A** is not necessarily uniaxial, but reflects the symmetry of a probe.

(16) Luckhurst, G. R. In *Liquid Crystals & Plastic Crystals*; Gray, G. W., Winsor, P. A., Ed.; Ellis Horwood: Chichester, England, 1974; pp 144–191.
(17) Saupe, A. *Z. Naturforsch.* **1964**, *19A*, 161.
(18) The outer doublet was difficult to analyze quantitatively. Judging from the unusually large spacing (more than twice that of the inner doublet) and the low intensity, these peaks seem to arise from the interaction involving azomethine protons.
(19) Fryburg, G. C.; Gelerinter, E. *J. Chem. Phys.* **1970**, *52*, 3378–3382.

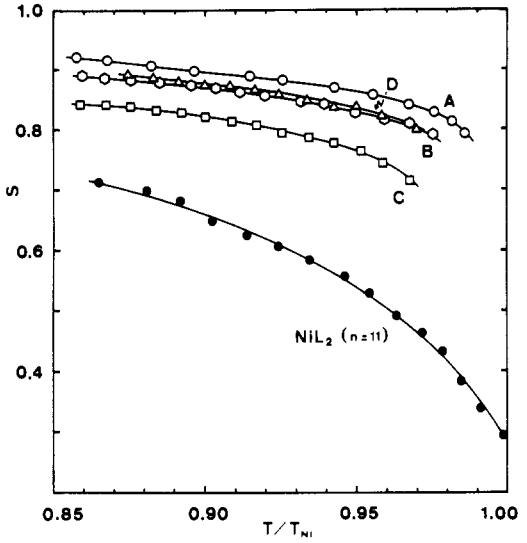

Figure 4. Orientational order parameters for long molecular axes of NiL_2 (n = 11) determined by NMR (solid circles) and of paramagnetic probes A–D in NiL_2 (n = 11) (open symbols) by ESR spectroscopies. The values were calculated by eq 7 with $\phi = 25°$ and by eq 9. Lines are only a guide for the eyes.

Table II. ESR Parameters for the Spin Probes[a]

probe	g	$g_\parallel$	$g_\perp$	a	$A_\parallel$	$A_\perp$
A	1.967	1.942	1.980	96.8	168.9	59.7
B	1.969	1.941	1.983	96.3	168.0	59.1
C	1.974	1.940	1.991	94.8	169.0	56.6
D	1.963	1.931	1.979	95.0	164.3	59.0

[a] Determined in *o*-terphenyl melts at 194–200 °C for isotropic parameters and in glasses at room temperature for parallel components; perpendicular components calculated from these data. Hyperfine constants are given in units of 10^{-4} cm^{-1}.

We assume for the time being, however, that A is axially symmetric and drop the third term in eq 8. Then the order parameter can be obtained from the ESR experiment by

$$\langle \Delta\nu \rangle_E - a = -(1/2)(A_{zz} - a)S \qquad (9)$$

where a and A_{zz} (or $A_\parallel$) can also be experimentally determined.

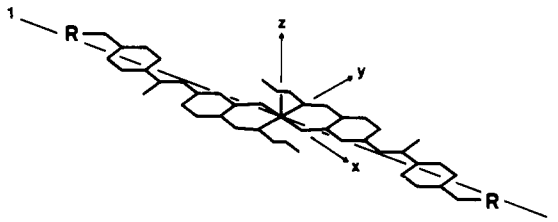

Oxovanadium(IV) probes of varied structures including VOL_2 (n = 11) and VOL_2 (n = 5) (probes A–D in Figure 5 and Table II) were subjected to the above ESR analysis. Actual spectra are exemplified by those for VOL_2 (n = 11) in NiL_2 (n = 11) in Figure 6. Small anisotropies in **g** tensors were neglected and the vanadium hyperfine spacings were measured (in gauss) directly from the outermost lines of the eight-line spectra. Figure 6 shows that when the sample is cooled, the separation of $7a \simeq 733$ G in the isotropic phase narrows down to $7\langle a \rangle = 507$ G at 184 °C and further to 471 G just before solidification. The data were analyzed only for the temperature range where spectral shape was well-defined as in Figure 6b. Molecular parameters a and $A_\parallel$ were determined separately in *o*-terphenyl melts and glasses, respectively, since presumably slower tumbling motion in the NiL_2 (n = 11) melt resulted in deformed spectral shape as in Figure 6a, which is not that of a purely isotropic state. Perpendicular branches of the glass spectra were rather complicated, but overall spectral shapes were of axial type for all of the probes.

The order parameters were calculated by eq 9 and plotted in Figure 4. It is easily seen that the values for the oxovanadium(IV)

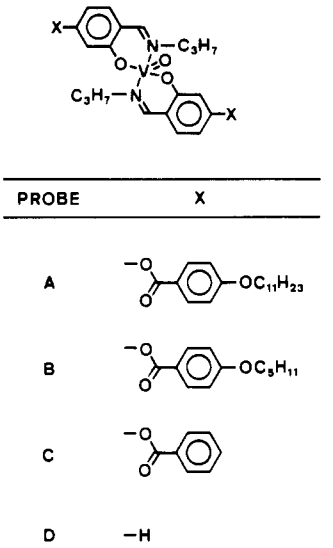

Figure 5. Structures for paramagnetic probes used in this study.

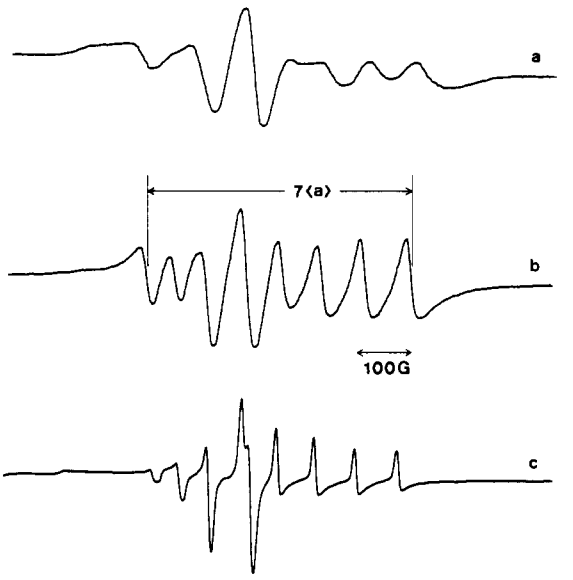

Figure 6. ESR spectral change with temperature of VOL_2 (n = 11) in NiL_2 (n = 11) just above T_{NI} (a) through just before solidification (c).

probes are invariably greater and less temperature dependent than those for the NiL_2 (n = 11) host. Since the probe concentrations are very small, the ESR results could be taken as those for NiL_2 (n = 11) in the cases of not only probes C and D but also A and B, which are mesogenic by themselves.

ESR measurements were repeated in *p*-azoxyanisole (PAA), a well-known nematogen, and the results are shown in Figure 7. The order parameters for this material fall between 0.4 and 0.6 for the given temperature range (T_{NI} = 136 °C). It shows that the orientational order of the probes in this nematic solvent increases as the probe molecules are elongated. Such a size effect on the solute alignment has been reported by Glarum and Marshall[20] for a variety of VO(β-diketonato)$_2$ complexes in PAA, and it has been demonstrated that larger molecules tend to be oriented better than the solvent itself. Therefore, a conventional nematic medium such as PAA does differentiate our probes as well according to the molecular size. In fact, this was a crux of the problem that led us to prepare metallomesogens so that paramagnetic probes would not be recognized as an impurity.

The apparent discrepancy between the NMR and ESR results for our metallonematogens may be partly accounted for by inherent ambiguities of the two methods, which are enlarged by unconventional characteristics of the new nematogens. The only

(20) Glarum, S. H.; Marshall, J. H. *J. Chem. Phys.* **1967**, *46*, 55–62.

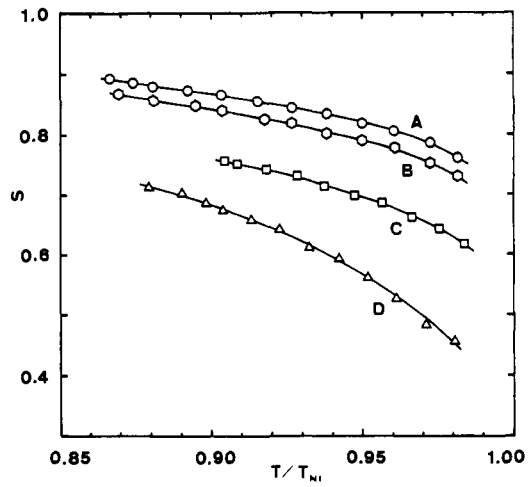

Figure 7. Orientational order parameters for long molecular axes of paramagnetic probes A–D in *p*-azoxyanisole. The values were calculated by eq 9. Lines are only a guide for the eyes.

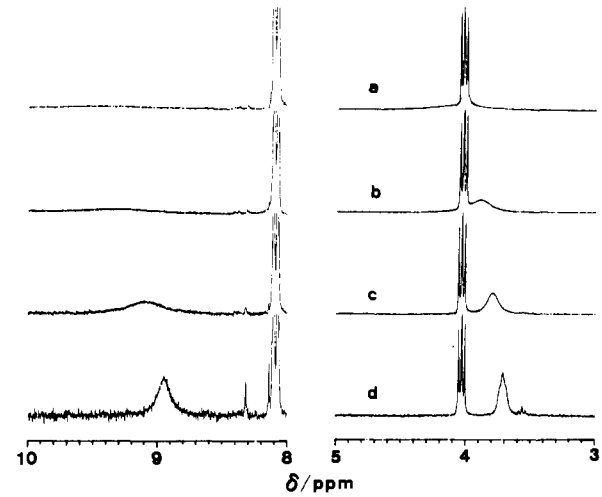

Figure 8. Concentration dependence of ^{1}H NMR spectra of NiL_2 (n = 11) in $CDCl_3$ showing broadening and downfield shift of azomethine (left) and *N*-methylene (right) signals with increasing concentration from ca. 2×10^{-3} M (d) through ca. 3×10^{-2} M (a).

ambiguity of the NMR method is in the estimate of ϕ, an angle between the interproton vector and the rotational axis. The value of S, calculated for $\phi = 25°$ is 0.293 at just below T_{NI} and gradually increases to 0.713 at $T/T_{NI} = 0.865$ (Figure 4), and these values are rather normal as nematic order parameters. Calculations for $\phi = 20°$ and 30°, however, yield profiles of S increasing from 0.260 to 0.633 and from 0.343 to 0.835, respectively, over the same temperature range. The uncertainty range is from −11 to +17%.

On the other hand, the assumptions regarding the principal axes of hyperfine tensors in the ESR approach involve a comparable amount of uncertainty. The hyperfine tensor has been determined for bis(*N*-methylsalicylaldiminato)oxovanadium(IV) doped in single crystals of its nickel(II) congener,[21] and in this case the A_{zz} direction was found to be tilted by about 10° away from the z axis defined for the nickel(II) host complex. If such steric repulsion against the V=O bond should be just as severe for our probes, the factor of $-1/2$ in eq 9 would be greater and in turn make S smaller by 9%. In addition, the third term in eq 8 vanishes either if the A′ tensor is cylindrically symmetric about the V=O axis or if the rotational symmetry axis bisects the two in-plane principal axes. These in-plane hyperfine axes lie very close to the Ni–O and Ni–N bond directions with an in-plane anisotropy of 11.3×10^{-4} cm^{-1} in the above case of doped crystals.[21] If complexes A–D are in a similar situation, even such a small difference ($A'_{xx} - A'_{yy}$ = 10 G, for instance) would make a significant contribution to the third term of eq 8 unless the l axis lies just between the x and y axes. The rotational axis appears to lie much closer to the V–O bond direction in our complexes substituted in the 4-position. An estimate for maximum possible uncertainty in S in the case of A'_{zz} = 82 G amounts to ±12%.

Another assumption of fast rotational motion around the l axis might not hold on the ESR time scale for our metallonematogens. If the average rotational potential does not have symmetry higher than 3-fold, the treatment as uniaxial nematics is not valid and the single scalar order parameter is insufficient to describe the orientational order. It has been shown that restricted motion of oxovanadium(IV) solutes in highly viscous liquid crystal solvents will result in apparently greater order parameters.[19] The asymmetric ESR line shapes observed for our complexes may correspond to this situation.

Given the above consideration of uncertainties, it still seems that the ordering of VOL_2 in NiL_2 is better than that of the latter alone. It should be recalled that the ESR measurements highlight the V=O centers, while the NMR information involve the whole core moiety of the molecule. A plausible explanation is that different parts of a molecule can yield different local order parameters[22] due to additional intramolecular motions, some site-specific intermolecular interactions, and so on, which are not taken into account in the above theoretical framework.

We also attempted ESR experiments using VO(β-diketonato)$_2$ probes in NiL_2 (n = 11) but apparent motional averaging occured only below ca. 160 °C with VO(dibenzoylmethanato)$_2$ and never reproducibly with VO(acetylacetonato)$_2$. On the other hand, two distinct species have been detected in a frozen solution of this chelate in *N*-(*p*-methoxybenzylidene)-*p*-*n*-butylaniline, another nematic liquid crystal,[23] suggesting a solvation phenomenon. It has been pointed out that spectral properties of the β-diketonate complexes of oxovanadium(IV) show a large solvent dependence, while β-ketoimine and salicylaldimine complexes do not.[24] The former species are susceptible to axial coordination at the sixth coordination site. A possibility remains, however, that similar interactions probably to a much lesser extent can affect properties of the present complexes of salicylaldimine derivatives.

Aggregation of NiL_2 in Solution. The NiL_2 (n = 11) complex yielded well-resolved ^{1}H NMR spectra in solution. We noticed, however, that the NMR signals from azomethine and *N*-methylene protons are highly concentration dependent. Their chemical shifts reported in the Experimental Section (8.94 and 3.71 ppm, respectively) are for a dilute solution of roughly 2×10^{-3} M in $CDCl_3$. They shift toward the downfield region with concomitant broadening as the solution becomes more concentrated, while the rest of signals remain unaffected (Figure 8). Both of these signals are nearly missing from the spectrum due to the extensive broadening for a solution about 15 times more concentrated. This behavior can be taken as an indication of aggregate formation in the solution phase.

Miyamura et al. have reported a study of the ^{1}H NMR peak shift and the paramagnetic broadening of [*N*,*N*′-bis(5-alkylsalicylidene)ethylenediaminato]nickel(II) in $CDCl_3$.[25] The concentration dependence of chemical shifts was observed for the azomethine proton and the one in the 6-position of the salicylidene unit of this Ni(salen) derivative, while the paramagnetic broadening (by an added copper analogue) was most noticeable for the azomethine and *N*-methylene protons. These combined results have led the authors to propose a dimeric structure for the associated species in which two molecules are stacked on top of each other in a centrosymmetric fashion.

(21) Hitchman, M. A.; Moores, B. W.; Belford, R. L. *Inorg. Chem.* **1969**, *8*, 1817–1820.

(22) Fringeli, U. P.; Schadt, M.; Rihak, P.; Gunthard, Hs. H. *Z. Naturforsch.* **1976**, *31A*, 1098–1107.

(23) Heppke, V. G.; Schneider, F. *Ber. Bunsen-Ges. Phys. Chem.* **1971**, *75*, 61–65.

(24) Fackler, Jr., J. T.; Levy, J. D.; Smith, J. A. *J. Am. Chem. Soc.* **1972**, *94*, 2436–2445.

(25) Miyamura, K.; Satoh, K.; Goshi, Y. *Bull. Chem. Soc. Jpn.* **1989**, *62*, 45–50.

In the present case of a bischelate type, however, axial association leading to generation of a paramagnetic metal center seems more likely. Stereochemistry of bis(*N*-*n*-alkylsalicylaldiminato)nickel(II) complexes was intensively studied for some time.[26] In the case of *N*-methyl derivative, for which molecular weight data over a range of concentrations indicated the association phenomenon[27] and also a fully paramagnetic isomer was isolated,[28] a polymeric (or at least dimeric in solution) structure involving axial coordination of donor oxygen atoms has been proposed. The partial paramagnetism of higher *N*-*n*-alkyl derivatives in inert solvents and in the molten state has also been reported,[29] and the pressure effect on the magnetic and spectral properties has been discussed in terms of the association equilibrium.[30] Therefore, if the substituents in the 4-position of the present *N*-*n*-propyl derivatives work in favor, such a scheme of axial coordination forming Ni-O···Ni linkages may apply to our NiL_2 complexes.

Such tendency might be extrapolated to the pure condensed phase; lathlike molecules of NiL_2 (n = 11) arranged in such a way could be regarded as a smectic-like group within the nematic domain. This kind of intermolecular interaction specific to the metal centers might affect the apparent orientational order probed by the ESR method. We would like to point out that the ^1H NMR relaxation time for NiL_2 (n = 11) in its nematic phase is roughly 0.1–0.2 s, which is shorter than that in its solid state at room temperature by an order of magnitude, although it is not certain whether this is due to a motional effect or to the paramagnetic influence. A magnetic susceptibility study of NiL_2 complexes is underway in order to clarify these points.

Experimental Section

Materials. Typical procedures for preparation of the complexes are given below.

Nickel(II) Complexes (NiL_2). 2,4-Dihydroxybenzaldehyde was subjected to DCC esterification[31] in its 4-position by an appropriate *p*-alkoxybenzoic acid,[5] and purified by several recrystallizations from methanol (or ethanol for higher homologues). A 2-mmol sample of the product was dissolved in a 70-mL quantity of hot methanol and allowed to react with 1 mmol of nickel acetate and then 2 mmol of *n*-propylamine by refluxing the mixture for 1–2 h. The resultant dark green solid was isolated by filtration, washed extensively with methanol, and purified by two or three recrystallizations from 2:1 methanol–chloroform mixtures. Yields: 70–90%, pale or dark green needlelike (n = 4–7), flaky (n = 9–12, and 14), or powdery (n = 8, 16, and 18) microcrystals. Anal. Found (calcd) for $C_{56}H_{76}N_2O_8Ni$ (n = 11): C, 69.71 (69.78); H, 8.05 (7.95); N, 2.92 (2.91). ^1H NMR ($CDCl_3$) for NiL_2 (n = 11): δ 8.94 (br s, 1 H, CH=N), 8.09 (d, J = 8.8 Hz, 2 H, benzoyl), 7.13 (d, J = 8.8 Hz, 1 H, salicylidene), 6.94 (d, 2 H, benzoyl), 6.37 (d, J = 2.2 Hz, 1 H, salicylidene), 6.31 (dd, 1 H, salicylidene), 4.03 (t, J = 6.6 Hz, 2 H, CH_2–O), 3.71 (br s, 2 H, CH_2–N), 1.91 (m, J = 7.1 Hz, 2 H, CH_2), 1.81 (m, J = 7 Hz, 2 H, CH_2), 1.52–1.27 (br m, 16 H, CH_2's), 1.01 (t, J = 7 Hz, 3 H, CH_3), 0.88 (t, J = 7 Hz, 3 H, CH_3).

Oxovanadium(IV) Complexes (VOL_2). Synthesis of VOL_2 followed an alternative route. 2-Hydroxy-4-(4-alkoxybenzoyloxy)benzaldehyde, prepared as above, was first condensed with *n*-propylamine.[10] A 2-mmol quantity of the isolated ligand was then reacted with $^1/_2$ equiv of vanadyl sulfate in methanol in the presence of triethylamine. A greenish solid formed immediately. After the mixture was refluxed for an hour, the product was collected and purified by induced crystallization from its chloroform solution by filtering, adding a saturating amount of methanol at its boiling point, and allowing it to cool down to room temperature. Yields: 40–60%, brownish gray powdery (n = 5–7, and 18), green needlelike (n = 8, 9, and 11), or flaky (n = 10, 12, 14, and 16) microcrystals with various tints. Anal. Found (calcd) for $C_{54}H_{72}N_2O_9V$ (n = 10): C, 68.86 (68.70); H, 7.71 (7.69); N, 3.02 (2.97).

Oxovanadium(IV) Complexes (C and D). The aldehyde component of the ligand in the above preparation was replaced by salicylaldehyde (for D) or its 4-benozyloxy derivative (for C) and the metalation was carried out without isolating the ligand, yielding dark green (C) and dark brown (D) microcrystals. Anal. Found (calcd) for $C_{34}H_{32}N_2O_7V$ (C): C, 64.64 (64.66); H, 5.08 (5.11); N, 4.49 (4.44). Found (calcd) for $C_{20}H_{24}N_2O_3V$ (D): C, 61.45 (61.38); H, 6.25 (6.18); N, 7.33 (7.16).

Physical Measurements. Calorimetric measurements were performed by using Rigaku Thermoflex, Rigaku TAS100, and DuPont 9900 differential scanning calorimeters. Heating or cooling rate was 5 K min^{-1}. High-resolution ^1H NMR spectra were recorded on a JEOL JNM-270 spectrometer at the Center of Instrumental Analysis, Hokkaido University. Dipolar splitting of the ^1H NMR line of neat NiL_2 (n = 11) was measured with an FT-NMR spectrometer operating at 29.8 MHz, locally constructed at Nihon University. The sample of NiL_2 (n = 11) was sealed in a 8-mm-o.d. Pyrex tube after evacuating for 30 h through a freeze–pump–thaw cycle. The X-band EPR spectra were recorded on a JEOL JES-FE1X spectrometer equipped with a high-temperature cavity controllable up to 200 °C. The samples were prepared in air by mixing a spin probe at a concentration no higher than 1 mol %.

Acknowledgment. This work was supported in part by Grants-in-Aid for Scientific Research Nos. 63740328 and 02854067 from the Ministry of Education, Science, and Culture of Japan. Support by the Japan Securities Scholarship Foundation and by the IMS Joint Studies Program (1989–1990) is also acknowledged.

(26) Holm, R. H.; O'Connor, M. J. *Progress in Inorganic Chemistry*; Wiley-Interscience: New York, 1971; Vol. 14, pp 241-401.
(27) Holm, R. H. *J. Am. Chem. Soc.* **1961**, *83*, 4683-4690.
(28) Harris, C. M.; Lenzer, S. L.; Martin, R. L. *Aust. J. Chem.* **1958**, *11*, 331-335.
(29) Sacconi, L.; Cini, R.; Ciampolini, M.; Maggio, F. *J. Am. Chem. Soc.* **1960**, *82*, 3487-3491.
(30) Ewald, A. H.; Sinn, E. *Inorg. Chem.* **1967**, *6*, 40-48.
(31) Hassner, A.; Alexanian, V. *Tetrahedron Lett.* **1978**, 4475-4478.

Notes

Contribution from the Department of Chemistry, Northwestern University, Evanston, Illinois 60208-3113

Synthesis and Structure of a New Ternary Telluride, $Cu_{1.85}Zr_2Te_6$

Patricia M. Keane and James A. Ibers*

Received December 28, 1990

Introduction

The known binary and ternary chalcogenides display unusual structural arrangements[1] and interesting physical properties.[2-4] The ternary systems of Nb and Ta involving sulfides,[5,6] selenides,[6-11] and more recently the tellurides[12-16] have been intensely

(1) Lévy, F. *Crystallography and Crystal Chemistry of Materials with Layered Structures*; Reidel Publishing Company: Dordrecht, Holland, and Boston, MA, 1976.
(2) Gamble, F. R.; DiSalvo, F. J.; Klemm, R. A.; Geballe, T. H. *Science* **1970**, *168*, 568.
(3) Delk, F. S.; Sienko, M. J. *Inorg. Chem.* **1980**, *19*, 1352-1356.
(4) Wilson, J. A. *Phys. Rev. B* **1979**, *19*, 6456-6468.
(5) Sunshine, S. A.; Ibers, J. A. *Inorg. Chem.* **1985**, *24*, 3611-3614.
(6) Meerschaut, A.; Gressier, P.; Guémas, L.; Rouxel, J. *Mater. Res. Bull.* **1981**, *16*, 1035-1040.
(7) Salem, A. B.; Meerschaut, A.; Guémas, L.; Rouxel, J. *Mater. Res. Bull.* **1982**, *17*, 1071-1079.
(8) Keszler, D. A.; Squattrito, P. J.; Brese, N. E.; Ibers, J. A.; Shang, M.; Lu, J. *Inorg. Chem.* **1985**, *24*, 3063-3067.
(9) Keszler, D. A.; Ibers, J. A. *J. Solid State Chem.* **1984**, *52*, 73-79.
(10) Keszler, D. A.; Ibers, J. A. *J. Am. Chem. Soc.* **1985**, *107*, 8119-8127.
(11) Sunshine, S. A.; Ibers, J. A. *Inorg. Chem.* **1986**, *25*, 4355-4358.
(12) Sunshine, S. A.; Keszler, D. A.; Ibers, J. A. *Acc. Chem. Res.* **1987**, *20*, 395-400.
(13) Liimatta, E. W.; Ibers, J. A. *J. Solid State Chem.* **1987**, *71*, 384-389.
(14) Liimatta, E. W.; Ibers, J. A. *J. Solid State Chem.* **1988**, *77*, 141-147.
(15) Liimatta, E. W.; Ibers, J. A. *J. Solid State Chem.* **1989**, *78*, 7-16.
(16) Mar, A.; Ibers, J. A. *J. Solid State Chem.*, in press.

0020-1669/91/1330-3096$02.50/0